Chinese Chemical Letters 35 (2024) 109102

Contents lists available at ScienceDirect

Chinese Chemical Letters

journal homepage: www.elsevier.com/locate/cclet

Tailored ionically conductive graphene oxide-encased metal ions for ultrasensitive cadaverine sensor

Ying Chen[a,1], Li Li[a,1], Junyao Zhang[a], Tongrui Sun[a], Xuan Zhang[a], Shiqi Zhang[c], Jia Huang[a,b,*], Yidong Zou[a,*]

[a] School of Materials Science and Engineering, Tongji University, Shanghai 201804, China
[b] Shanghai Key Laboratory of Anesthesiology and Brain Functional Modulation, Translational Research Institute of Brain and Brain-Like Intelligence, Shanghai Fourth People's Hospital Affiliated to Tongji University, Tongji University, Shanghai 200434, China
[c] School of Mechanical Engineering, Nantong University, Nantong 226019, China

ARTICLE INFO

Article history:
Received 24 July 2023
Revised 26 August 2023
Accepted 14 September 2023
Available online 16 September 2023

Keywords:
Graphene oxide
Cadaverine monitoring
Chemical sensor
Ionically conductive
Homogeneity

ABSTRACT

Intelligent chemical sensors have been extensively used in food safety and environmental assessment, while limited sensitivity and homogeneity bring about huge obstacles to their practical application. Herein, novel ionically conductive sensitive materials were elaborately designed based on metal ion decorated graphene oxide (GO) *via* a facile and general *in-situ* spin-coating strategy, where the abundant functional groups (-OH and -COOH) of GO layer could provide natural binding sites for various bivalent metal cations (such as Cu^{2+}, Ni^{2+}, Zn^{2+}, Co^{2+}, and Mg^{2+}) through coordination and electrostatic interaction. The intercalated metal cations on the layered GO nanosheets can be regarded as charge carriers and complexation with targeted gas (cadaverine, Cad), which is a typical metabolites production and food degradants. By contrast, the designed GO@Cu(II) sensor exhibited the optimal sensing performance toward Cad molecules at room temperature, including ultra-low detection limit (*ca.* 3 nL), excellent sensitivity, and rapid low concentration detection rate (only 16 s). Interestingly, the sensor exhibited an irreversible and specific response toward Cad, while it showed a transient and reversible response to other interfering gases, implying its outstanding selectivity. In addition, the GO@Cu(II) sensor enabled real-time monitoring of the decay progression of cheese, and it exhibited great potential for large-scale production *via* its excellent homogeneity. It provides an efficient approach to tailoring intelligent chemical sensors for real-time food safety monitoring and human health warning.

Recently, cadaverine (Cad, 1,5-pentanediamine) as a degradation product of lysine has been widely regarded as an important bioactive indicator to reflect physiological activities, including gene expression, cell growth, proliferation, *etc.* [1–3]. However, high concentrations of Cad can cause serious security threats to human health, such as respiratory diseases, immune system disorders, and central nervous system damage [4]. Besides, Cad is frequently found in various foods such as fish, eggs, milk, and meat [5,6], and improper processing or storage will result in a dramatic increase in the level of Cad in food, which will lead to severe food poisoning [7,8]. Especially, it has been demonstrated that Cad is detrimental to the recovery of periodontal inflammation and is also strongly associated with the formation of various cancers [9,10]. Therefore, it is of great significance for human food safety and physical health to achieve highly sensitive and selective detection of Cad.

Endless analytical methods have been applied for the detection of Cad, such as electrochemical analysis and chromatographic techniques [11], and the latter is the most commonly used method for the detection of Cad in food, including thin-layer chromatography [12], ion-pair liquid chromatography [13], gas chromatography [14], and high-performance liquid chromatography [15]. Although these methods are efficient, precise, and feasible for the detection of trace analytes, all of them are limited in practical applications by their bottlenecks, such as extensive pretreatment, time-consuming, high reagent consumption, specialized large equipment, and skilled personnel [16–20]. Thus, it is difficult to realize rapid, convenient, environmentally friendly, and low-cost real-time detection of Cad through the existing technology.

In contrast, chemical sensors exhibit unprecedented application advantages and unique performance for gas monitoring, which

* Corresponding authors at: School of Materials Science and Engineering, Tongji University, Shanghai 201804, China.
E-mail addresses: huangjia@tongji.edu.cn (J. Huang), ydzou@tongji.edu.cn (Y. Zou).
[1] These authors contributed equally to this work.

https://doi.org/10.1016/j.cclet.2023.109102
1001-8417/

are dependent on the electrical signal variation of sensing devices [21–23]. Most of them are mainly dependent on the surface oxidation–reduction reactions and electron mobility between electronically conductive materials and target analytes [24–26], which possess a wide detection range and good stability but suffer from low sensitivity and poor selectivity. In addition, these electronically conductive sensitive materials such as metal oxides and noble metals, which employ electrons or holes as charge carriers, usually require high operating temperatures to promote the interface catalytic reaction, inevitably generating higher energy consumption [27]. By contrast, most ionically conductive materials such as hydrogels have been regarded as efficient sensitive materials for flexible pressure and strain sensors, which can convert mechanical deformation into detectable electrical signals [28–30]. Interestingly, these attracted ionically conductive materials can be also considered as potential responsive materials for gas sensors based on the greater component diversity and abundant interaction modes with target analytes, which can significantly improve sensing sensitivity and selectivity. For example, novel ionically conductive metal-organic frameworks (IC-MOFs) based on metal ions as charge carriers can be employed as active materials to fabricate chemical sensors with excellent selectivity and sensitivity due to the unique interaction between the ion charge carrier and the analyte, illustrating the great potential of ion carriers for chemical gas sensing [31–33]. Therefore, it is valuable and essential for food safety monitoring to develop novel ionically conductive Cad sensors with high sensing performance, good uniformity, and easy scalability.

Graphene oxide (GO) as a two-dimensional flexible star material has been considered as a promising candidate for long-term applications in the field of sensors due to its excellent physicochemical properties, including large specific surface area, abundant oxygenated functional groups, and superior hydrophilicity [34–37]. In addition, it is easy to assemble and functionalize with various components, such as metal ions, alkyl chains, peptides, antibodies, and proteins [38–41]. Due to its high surface area, it can effectively disperse adhering materials and prevent agglomeration during compounding with metals, metal oxides, polymers, or other materials. Therefore, it is attainable to load various metal ions *via* the coordination and electrostatic interaction between functional groups of negative GO (*e.g.*, -OH and -COOH) and positive metal ions.

Herein, a novel and general spin-coating strategy was proposed to design metal ion-decorated GO-based chemical sensors with metal ions as sensing charge carriers. The enriched metal ions can freely intercalate among layered GO and migrate under alternating current (AC) voltage to achieve ionic conductive properties. In addition, the abundant oxygen-containing groups and anchored metal cations can provide advantaged adsorption sites for targeted gas molecules. In order to evaluate the effect of various metal cations (*i.e.*, Cu^{2+}, Ni^{2+}, Zn^{2+}, Co^{2+}, and Mg^{2+}), a series of GO-metal ions composites (GO@M(II)) have been synthesized and employed as sensitive layers to *in-situ* fabricate versatile gas sensors with low power consumption. It was found that GO@Cu(II) exhibited the optimal sensing capability toward Cad molecules, including high sensitivity (84.6% *vs.* 1 μL), excellent selectivity, fast response rate (*ca.* 16 s), low detecting volume (0.02 μL) and ultralow theoretical detection limit (3 nL). In addition, the sensors exhibited an irreversible and specific response to Cad while a transient and reversible response to other interfering components, implying its excellent selectivity. Especially, it showed good homogeneity and reproducibility *via* mass device preparation and parallel experiments. These exposed metal cations can directly interact with the target analytes through a strong complex interaction, and this strategy endows the sensor with the advantages of easy and low-cost fabrication, as well as superior consistency among devices.

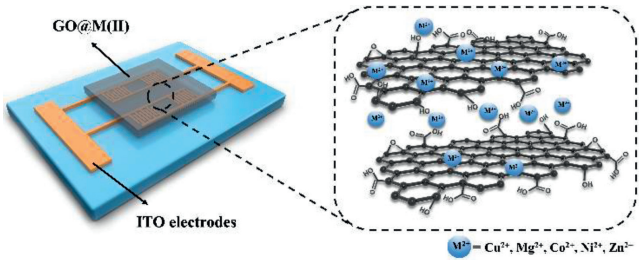

Scheme 1. Schematic diagram of the *in-situ* integrated GO@M(II) sensor and the structure of the sensing layer.

Novel metal ions incorporated GO film hybrid sensors were designed *via* a facile spin-coating method at room temperature, which was suitable for mass production with low cost and high yields (Scheme 1). The sensitive layers were fabricated on a substrate etched with indium tin oxide (ITO) interdigital electrodes based on GO nanosheets and metal nitrate aqueous solution, and active sensing layer GO@M(II) (M(II): Cu^{2+}, Ni^{2+}, Zn^{2+}, Co^{2+}, and Mg^{2+}) was *in-situ* growth on the surface of electrodes by general spin-coating technique. With the assistance of oxygenated abundant functional groups (*i.e.*, -OH and -COOH) and the hydrophilic surface of GO nanosheets, the positively charged bivalent metal cations can be evenly dispersed and incorporated on the negatively charged GO nanosheets through coordination or electrostatic interaction [42]. In addition, GO nanosheets can be regarded as favorable flexible substrate and ion carriers' transmission medium, and loaded metal ions can migrate freely among GO nanosheet layers under AC voltage. Thus, the tailored ionically conductive GO@M(II) can be utilized as efficient sensing materials with metal ions as charge carriers for real-time detecting targeted analytes.

To evaluate the structure property of as-prepared GO@M(II) materials, taking GO@Cu(II) as an example, the chemical state of C, O, and Cu elements were collected from the X-ray photoelectron spectroscopy (XPS) analysis. The C 1s spectrum of GO@Cu(II) can be divided into four typical peaks [43], and the peak associated with the C-O bond displays a significant shift and change in relative intensity than that in pure GO (Figs. 1a and b). The intensity of the peak related to C-O bond decreased sharply from 34.73% of GO to 5.98% of GO@Cu(II), and it was ascribed to that the oxygen-containing functional groups (-OH and -COOH) of negatively charged GO combined with Cu^{2+} cations. In addition, the peak corresponding to C=O bond also weakened, which was attributed to that the introduced Cu^{2+} ions could adjust the coordination environment of C and O atoms (Table S1 in Supporting information) [44,45]. Interestingly, the O 1s spectrum of GO@Cu(II) showed a similar but shifted to a higher binding energy than that of GO (Fig. 1c), which was attributed to that GO with abundant -OH and -COOH groups could possess the function of the Lewis-base and the Cu^{2+} ions employ as Lewis-acid. Thus, the delocalized π-electron systems of GO could interact with Cu^{2+} ions to produce electron donor-acceptor complexes [46,47]. It further implies that the introduction of Cu^{2+} ions changes the coordination form of O atoms. GO@Cu(II) also showed new characteristic peaks in Cu 2p spectrum (Fig. 1d), and these results indicated that the Cu^{2+} ions could interact with the GO nanosheets to form composite materials. It showed typical characteristic peaks of Cu $2p_{1/3}$ and Cu $2p_{2/3}$, and the binding energy of Cu $2p_{2/3}$ was about 935.8 eV, which indicated that the most impregnated Cu^{2+} ions existed in the typical metallic state. The coexistence and homogeneous distributions of Cu, O, and C elements were confirmed through the energy dispersive spectroscopy (EDS) elemental mapping (Figs. 1e and f). It could be clearly seen that the Cu species were uniformly

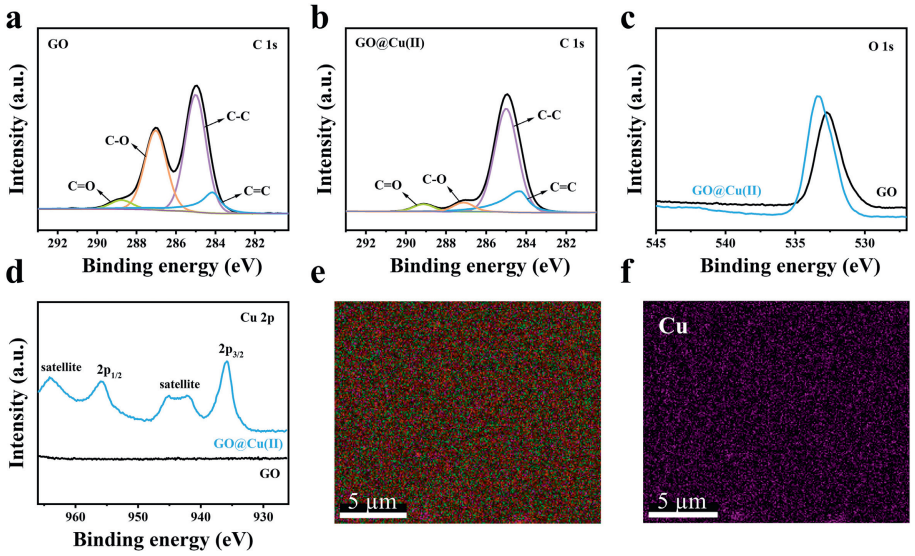

Fig. 1. The C 1s XPS spectra of (a) GO and (b) GO@Cu(II). The (c) O 1s and (d) Cu 2p spectra of GO and GO@Cu(II). The EDS mapping of (e) GO@Cu(II) and (f) Cu-K, demonstrates the uniform distribution of Cu element.

distributed on the GO substrate, which further demonstrated the successful loading of Cu^{2+} ions.

Benefitting from the above unique properties, the as-prepared GO@M(II) have been applied as sensitive materials to design gas sensors for Cad detecting. Due to the presence of abundant metal ions in the GO substrate, metal cations become the main carriers of charge rather than traditional electrons or holes [31,33]. Therefore, the sensing device can possess a stable capacitance at AC voltage, and the relative capacitance change of the device is employed as the signal output for the detection of targeted species. The whole test was carried out in a homemade apparatus, where the device was placed in a manual chamber and connected to a TH2827C Precision LCR Meter. All detection signals were collected by the LCR Meter, and the test was performed in an atmospheric environment with an operating voltage of 1 V and a frequency of 400 Hz. When the capacitance of the sensor stabilizes to reach the relatively smooth baseline, a volume of Cad solution is introduced into the chamber to evaporate into vapor. Once the sensing layer contact with Cad molecules, the capacitance of the sensor will change to generate a detection signal instantly. Afterward, the air was allowed into the chamber to gradually dilute and purge the Cad gas. The capacitance of the sensor is finally stabilized, and the difference between the final value and the initial one is the irreversible response signal to Cad species.

In order to evaluate the unique sensing behavior of GO@M(II), the response performance of the sensing devices toward Cad gas was evaluated *via* batch experiments. The real-time response curves of the sensors based on five different metal cations for a specific volume of Cad (Figs. S2 and S3 in Supporting information) show that all sensitive materials have a relatively fast response rate. As shown in Table S2 (Supporting information), these sensors exhibit a relatively short response time within 40 s, where the GO@Mg(II) and GO@Cu(II) possess the fastest response rate with 15 s and 16 s, respectively. By contrast, the sensors with copper ions as charge carriers have a higher average response level of 7.5% (0.1 μL) and 84.6% (1 μL), respectively (Figs. 2a and b), which is obviously superior to other metal ion-based sensors. A comparison of the cumulative stability constants of several metal-ethylenediamine complexes reveals that the copper-ethylenediamine complex has the largest cumulative stability constant, implying the optimal binding capacity between Cu species and Cad molecules [33], which is consistent with the

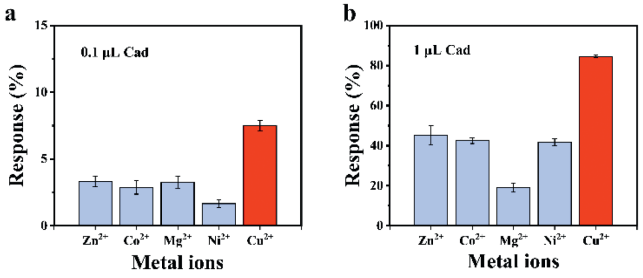

Fig. 2. Response of GO@M(II) sensors based on different metal ions (Zn^{2+}, Co^{2+}, Mg^{2+}, Ni^{2+}, and Cu^{2+}) to (a) 0.1 and (b) 1 μL of Cad at room temperature, respectively.

sensing experimental results. Thus, it shows that copper ions have a greater tendency to complex with Cad and generate more stable complexes compared to other ions, thus presenting superior sensing sensitivity.

In order to further evaluate the sensing behavior of GO@Cu(II)-based sensors, the response of the sensors toward Cad with various concentrations (0.02, 0.06, 0.1, 0.2, 0.4, 0.6, 0.8, and 1 μL, respectively) were mainly examined. The real-time response plot of the sensor to 1 μL of Cad shows that it has a fast response with a response time of only 16 s (Fig. 3a). The response process of the devices exhibited a fast response rate for all concentrations of Cad and could sensitively capture trace Cad gas (Fig. 3b and Fig. S1 in Supporting information). As shown in Table S3 (Supporting information), the sensor exhibited a fast response rate (<25 s) under the above concentrations, which was mainly due to the competitive adsorption and saturation of reaction sites under various concentrations. It was attributed to the large specific area of GO nanosheets, abundant Cu^{2+} ions, and active surface groups, which could provide a large number of adsorption and binding sites for Cad molecules [48,49]. Interestingly, an average response of 3.49% was achieved even for 0.02 μL Cad, and it indicated that the tailored sensors could be employed to detect Cad gas with ultra-low concentration. A curve with high linearity is obtained by fitting the responses under various concentrations from 0.02 μL to 1 μL, which indicates that the sensor has a good linear relationship between sensing response and Cad concentration (Fig. 3c). In addition, the error bar was also relatively small and within the allow-

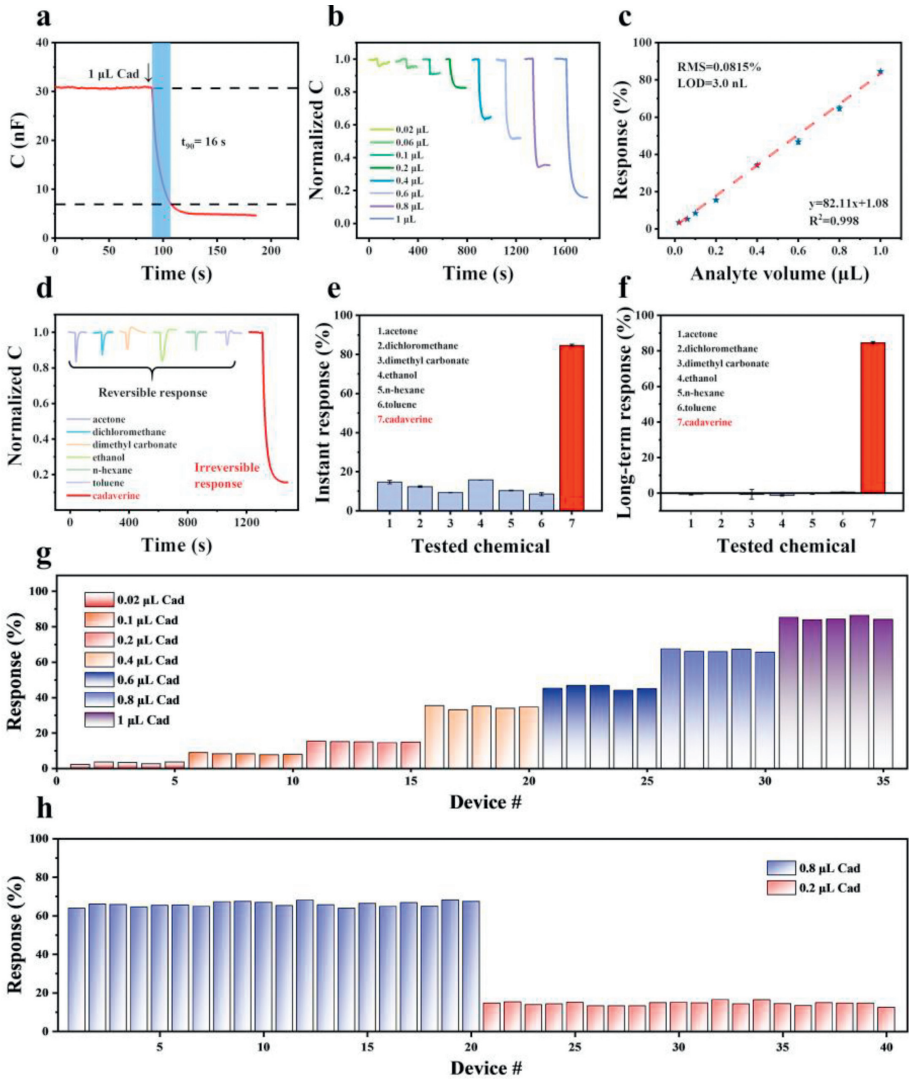

Fig. 3. (a) Real-time response curve of the GO@Cu(II) sensor to 1 μL of Cad at room temperature. (b) Normalized capacitance response curves of GO@Cu(II) sensors to different volumes of Cad (0.02, 0.06, 0.1, 0.2, 0.4, 0.6, 0.8, and 1 μL) at room temperature. (c) The plot of the response of GO@Cu(II) sensors to different volumes of Cad. (d) Normalized capacitance response, (e) instant responsivity, and (f) long-term responsivity of GO@Cu(II) sensors to different volatile organic compounds at room temperature. (g) Response of 35 GO@Cu(II) sensors to different volumes of Cad at room temperature. (h) Response of 40 GO@Cu(II) sensors to Cad, with 20 of them to 0.2 μL of Cad and the remaining to 0.8 μL at room temperature.

able error range, demonstrating excellent consistency among these sensor devices. In addition, the theoretical minimum detection limit (LOD) was calculated to be about 3 nL based on the classical theory formulas, which suggested that the sensors had great potential to detect Cad gas under extremely low concentrations.

Besides, achieving high selectivity for the specific analyte still remains a huge challenge for chemical sensors. To estimate the selectivity of GO@Cu(II) toward Cad gas, the sensors were performed under various interference gasses (Fig. 3d and Fig. S4 in Supporting information), including acetone, dichloromethane, dimethyl carbonate, ethanol, *n*-hexane, and toluene. It illustrates the real-time response of the device to various volatile chemical analytes. The same volumes (1 μL) of chemicals such as ethanol and acetone were injected into the chamber, respectively, and the capacitance of the sensor device rapidly decreased upon contact with these gases, but it quickly returned to its original value. The sensors showed a lower response to all of these common volatile interference gases and exhibited a reversible response. In contrast, when the sensor device was exposed to Cad gas, the capacitance rapidly decreased and then never recovered, exhibiting a significant and irreversible response. This reversible-irreversible response difference is due to that Cu^{2+} ions can react with Cad molecules to form stable coordination compounds with poor decomposability *via* the strong coordination interaction. However, owing to the weak physical adsorption and lower complexation stability constant among Cu^{2+} ions and these volatile chemical analytes, the sensor can adsorb and desorb the above gasses to form reversible reactions. In view of the transient response (Fig. 3e), the response toward Cad of 1 μL was 84.6%, which was more than 4 times higher than that for other chemical gasses (response less than 20%). Interestingly, after the response signal was stabilized, the sensor exhibited a negligible response to the other chemical gasses (close to zero), while the response to Cad was still maintained and irreversible (Fig. 3f). It demonstrates that the GO@Cu(II)-based sensor has high selectivity and can accurately identify Cad gas in complex environments with interference from other common chemical vapors. The higher selectivity of GO@Cu(II) toward Cad can be ascribed to the strong coordination interaction between Cad and active Cu^{2+} cations, which can form stable coordination compounds to avoid desorption. Based on the unique irreversible recognition, it

can be regarded as an irreplaceable sensitive material for a smart early-warning instrument in safety monitoring and food detection.

Generally, device homogeneity is an important indicator to verify the operational stability and assay reproducibility of the sensor devices [50,51]. In order to evaluate the stability and consistency of the sensors, mass experiments are performed to systematically investigate the superiority of the device preparation strategy. It can be seen that most of the parallel devices show similar responses to the same volume of Cad with negligible discrepancy (Fig. 3g), indicating that the devices exhibit good homogeneity. In addition, with the increase of Cad concentration, the corresponding response showed an excellent linear relationship. In addition, taking 0.2 μL and 0.8 μL as an example, the response of the sensors to the same volume of Cad was further studied. The bar chart directly illustrated the response of 40 devices to Cad (Fig. 3h), 20 of which were exposed to 0.2 μL of Cad and 20 to 0.8 μL of Cad, respectively. The devices showed negligible change in response to the same volume of Cad, with an average response of 14.5% ± 0.98% for 0.2 μL of Cad, and an average response of 66.0% ± 1.28% for 0.8 μL of Cad, respectively. A comparison of the sensing performance between GO@Cu(II)-based sensors and other reported sensors is presented in Table S4. Compared to other sensing materials, such as enzymes, dyes, nanoparticles, polymers, and metal oxides, the GO@Cu(II) displayed a much shorter response time than most of them, as well as a comparable LOD value. It exhibited that the as-prepared sensitive materials were endowed with superior sensing performance, and it was expected to provide important candidate materials and devices for practical applications.

To explore the practical application of GO@Cu(II)-based sensor, it was applied to real-time monitor Cad gas from the decay progression of commonly used cheese (Fig. 4a). The sensor device was placed in a homemade chamber, which fixed an appropriate amount of cheese on a glass lid at a certain height. The sensor device containing cheese was placed in an environment with constant temperature (25 °C) and humidity (55%). During a period of over 2000 min, the capacitance of the device gradually decreased to 6% of its original value as the cheese decayed, indicating that the sensor could sensitively detect the presence of Cad gas in the environment and reflect trace changes of concentration (Fig. 4b). Thus, it confirms that the GO@Cu(II)-based sensor has promising potential for real-time monitoring of Cad gas in practical applications.

Furthermore, in order to investigate the sensing mechanism of Cad detection, the ion conduction property of the sensing device was verified and the surface chemical state of the sensing layer before and after exposure to Cad was also analyzed *via* XPS technique. As shown in Fig. 4c, a certain positive or negative direct voltage was applied to the sensor alternately. When a positive voltage was applied to these sensors, the current through the sensors rapidly decreased. Similarly, when the voltage was negative, the reverse current also decayed rapidly, indicating that metal ions were capable of migrating back and forth between the electrodes. In addition, comparing the N 1s spectra of GO@Cu(II) before and after the detection of Cad (Fig. 4d), it can be seen that two new peaks (400.7 and 398.9 eV) appeared after the detection of Cad, which are corresponding to N-Cu and N-C bonds, respectively [52–54]. A schematic diagram of the sensing mechanism is illustrated in Fig. 4e. During the sensing process, Cad molecules could form stable complexes with freely moved Cu^{2+} ions, which inhibited the migration of Cu^{2+} ions and led to a decrease in the capacitance of the sensor. Especially, since the complexes were relatively stable and not easily decomposed, and it showed an irreversible response toward Cad gas.

In conclusion, novel and efficient GO@M(II) chemical sensors based on different metal ions (*i.e.*, Cu^{2+}, Ni^{2+}, Zn^{2+}, Co^{2+}, and Mg^{2+}) as charge carriers were designed and tailored *via* a simple spin-coating method, where the GO@Cu(II)-based sensor exhibited

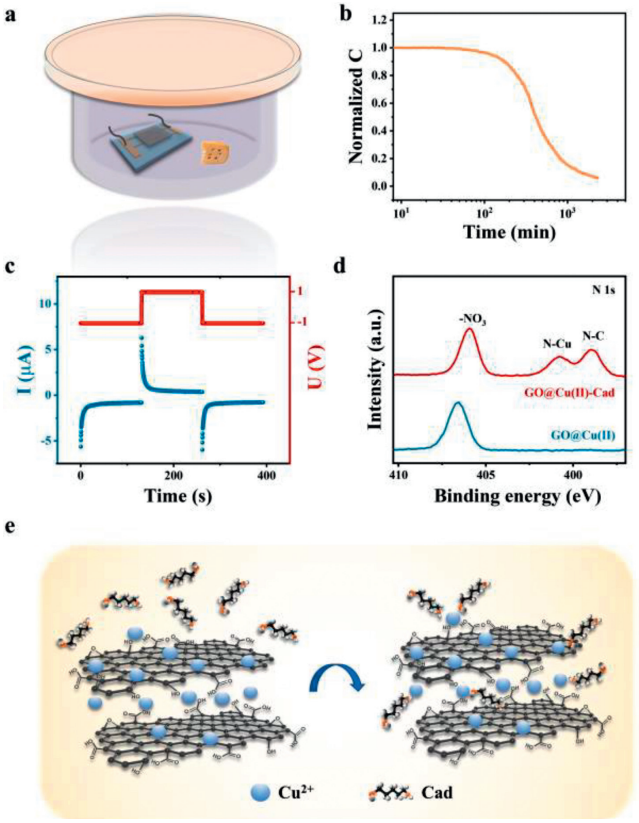

Fig. 4. (a) Schematic diagram of the device for monitoring the decay of cheese. (b) Normalized response curve of the GO@Cu(II) sensor for cheese decay at room temperature. (c) The *I-T* curve of ionic properties of the GO@Cu(II) sensor. (d) The N 1s XPS spectra of the GO@Cu(II) sensor before and after the detection of Cad. (e) Schematic diagram of the sensing mechanism towards Cad of the GO@Cu(II) sensor.

the optimal sensing performance toward Cad gas at room temperature. It can rapidly detect trace Cad gas with a rapid response rate of only about 16 s, and it can also accurately recognize Cad gas even under very low concentration (0.02 μL in volume) with an ultralow theoretical minimum detection limit (3 nL). Interestingly, it presented a distinctive and permanent response to Cad gas, while showing a temporary and reversible response to other common volatile interfering gasses. It enabled real-time monitoring of the trace Cad gas with high sensitivity and selectivity in complex scenarios. Importantly, the homogeneity of the sensor device was outstanding, and the sensor device was simply prepared, cost-effective, and user-friendly, and thus it was very suitable for mass production. The excellent sensing performance of GO@Cu(II)-based sensor provides a promising candidate for real-time monitoring of Cad, and it opens up a new door in the development of smart sensors for food safety monitoring.

Declaration of competing interest

The authors declare no competing financial interest.

Acknowledgments

This work was supported by the National Natural Science Foundation of China (Nos. 62074111, 22105043), the Science & Technology Foundation of Shanghai (Nos. 19JC1412402, 20JC1415600), Shanghai Municipal Science and Technology Major Project (No. 2021SHZDZX0100), Shanghai Municipal Commission of Science and Technology Project (No. 19511132101), and the support of the Fundamental Research Funds for the Central Universities.

The authors also thank the characterization and testing center of School of Materials Science and Engineering at Tongji University for materials characterization.

Supplementary materials

Supplementary material associated with this article can be found, in the online version, at doi:10.1016/j.cclet.2023.109102.

References

[1] K.B. Biji, C.N. Ravishankar, R. Venkateswarlu, et al., J. Food Sci. Technol. 53 (2016) 2210–2218.
[2] A. Halasz, A. Barath, L. Simonsarkadi, et al., Trends Food Sci. Technol. 5 (1994) 42–49.
[3] A. Hussain, L.R. Saraiva, D.M. Ferrero, et al., Proc. Natl. Acad. Sci. U. S. A. 110 (2013) 19579–19584.
[4] H. Yang, D. Kim, J. Kim, et al., ACS Nano 11 (2017) 11847–11855.
[5] C. Ruiz-Capillas, F. Jimenez-Colmenero, Crit. Rev. Food Sci. Nutr. 44 (2004) 489–499.
[6] H. Vasconcelos, J.M.M.M. de Almeida, A. Matias, et al., Trends Food Sci. Technol. 113 (2021) 86–96.
[7] C. Ruiz-Capillas, A.M. Herrero, Foods 8 (2019) 62.
[8] J.H. Mah, Y.K. Park, Y.H. Jin, et al., Foods 8 (2019) 85.
[9] L. Prester, Food Addit. Contam. Part A Chem. Anal. Control Expo. Risk Assess. 28 (2011) 1547–1560.
[10] A.K. Handa, T. Fatima, A.K. Mattoo, Front. Chem. 6 (2018) 10.
[11] A. Onal, Food Chem. 103 (2007) 1475–1486.
[12] A. Romano, H. Klebanowski, S.La Guerche, et al., Food Chem. 135 (2012) 1392–1396.
[13] J. Sun, H.X. Guo, D. Semin, et al., J. Chromatogr. A 1218 (2011) 4689–4697.
[14] C. Almeida, J.O. Fernandes, S.C. Cunha, Food Control 25 (2012) 380–388.
[15] M. Ishimaru, Y. Muto, A. Nakayama, et al., Food Anal. Methods 12 (2019) 166–175.
[16] C. Proestos, P. Loukatos, M. Komaitis, Food Chem. 106 (2008) 1218–1224.
[17] C. Basheer, W. Wong, A. Makahleh, et al., J. Chromatogr. 1218 (2011) 4332–4339.
[18] I. Basozabal, A. Gomez-Caballero, G. Diaz-Diaz, et al., J. Chromatogr. 1308 (2013) 45–51.
[19] J. Donthuan, S. Yunchalard, S. Srijaranai, J. Sep. Sci. 37 (2014) 3164–3173.
[20] R.M. Ramos, I.M. Valente, J.A. Rodrigues, Talanta 124 (2014) 146–151.
[21] Y. Chen, Y. Li, B. Feng, et al., Sens. Actuator. B: Chem. 360 (2022) 131662.
[22] Z. Zhu, H. Liu, P. Ding, et al., ACS Sens. 8 (2022) 1318–1327.
[23] B. Feng, Y. Wu, Y. Chen, et al., ACS Appl. Nano Mater. 5 (2022) 9688–9697.
[24] P. Ding, H. Liu, Z. Zhu, et al., ACS Sens. 8 (2022) 2375–2382.
[25] Z. Yuan, M. Bariya, H.M. Fahad, et al., Adv. Mater. 32 (2020) 1908385.
[26] T. Kim, T.H. Lee, S.Y. Park, et al., ACS Nano 17 (2023) 4404–4413.
[27] X. Yang, Y. Deng, H. Yang, et al., Adv. Sci. 10 (2023) 2204810.
[28] L. Wang, G. Gao, Y. Zhou, et al., ACS Appl. Mater. Interfaces 11 (2019) 3506–3515.
[29] R.L. Truby, M. Wehner, A.K. Grosskopf, et al., Adv. Mater. 30 (2018) 1706383.
[30] M.S. Sarwar, Y. Dobashi, C. Preston, et al., Sci. Adv. 3 (2017) e1602200.
[31] L. Li, S. Zhang, Y. Lu, et al., Adv. Mater. 33 (2021) e2104120.
[32] Y. Lu, S. Zhang, S. Dai, et al., Matter 3 (2020) 904–919.
[33] S. Zhang, L. Li, Y. Lu, et al., J. Mater. Chem. C 10 (2022) 5497–5504.
[34] G. Jiang, M. Goledzinowski, F.J.E. Comeau, et al., Adv. Funct. Mater. 26 (2016) 1729–1736.
[35] D. Lei, Q. Zhang, N. Liu, et al., Adv. Funct. Mater. 32 (2022) 2107330.
[36] G. Eda, M. Chhowalla, Adv. Mater. 22 (2010) 2392–2415.
[37] Y. Zhu, S. Murali, W. Cai, et al., Adv. Mater. 22 (2010) 3906–3924.
[38] W. Yu, L. Sisi, Y. Haiyan, et al., RSC Adv. 10 (2020) 15328–15345.
[39] X.Q. Wei, L.Y. Hao, X.R. Shao, et al., ACS Appl. Mater. Interfaces 7 (2015) 13367–13374.
[40] O.C. Compton, S.T. Nguyen, Small 6 (2010) 711–723.
[41] T. Ramanathan, A.A. Abdala, S. Stankovich, et al., Nat. Nanotechnol. 3 (2008) 327–331.
[42] Y. Long, K. Wang, G. Xiang, et al., Adv. Mater. 29 (2017) 1606093.
[43] N. Boulanger, A.S. Kuzenkova, A. Iakunkov, et al., ACS Appl. Mater. Interfaces 12 (2020) 45122–45135.
[44] P. Vazquez-Sanchez, M.A. Rodriguez-Escudero, F.J. Burgos, et al., J. Alloy. Compd. 800 (2019) 379–391.
[45] T. Kuilla, S. Bhadra, D. Yao, et al., Prog. Mater. Sci. 35 (2010) 1350–1375.
[46] Y. Ma, W. Shao, W. Sun, et al., Appl. Surf. Sci. 459 (2018) 544–553.
[47] A.S.K. Kumar, S. Jiang, J. Mol. Liq. 237 (2017) 387–401.
[48] D.H. Carrales-Alvarado, I. Rodriguez-Ramos, R. Leyva-Ramos, et al., Chem. Eng. J. 402 (2020) 126155.
[49] S. Yang, L. Li, Z. Pei, et al., Carbon 75 (2014) 227–235.
[50] M. Deng, Z. Li, X. Deng, et al., J. Mater. Sci. Technol. 164 (2023) 150–159.
[51] X. Liu, J. Ma, P. Jiang, et al., ACS Appl. Mater. Interfaces 12 (2020) 45332–45341.
[52] B. Tan, B. Xiang, S. Zhang, et al., J. Colloid Interface Sci. 582 (2021) 918–931.
[53] W. Li, W. Luo, X. Yu, et al., J. Mol. Liq. 357 (2022) 119110.
[54] Z. Liu, Q. Chu, H. Chen, et al., Colloids Surf. A 669 (2023) 131504.